Drop impact formed vortex rings

Muhammad Saeed Saleem
Master student (2017-2019)
Xi'an Jiaotong University

Nathan BLANKEN, Hossain Chizari, Marie-Jean THORAVAL
Basilisk/Gerris Users' Meeting 2019
18 June 2019

Background: Drop impact on a pool of same liquid

Increasing Impact velocity

Bouncing Droplet
- Velocity = 0.31 ms^{-1}

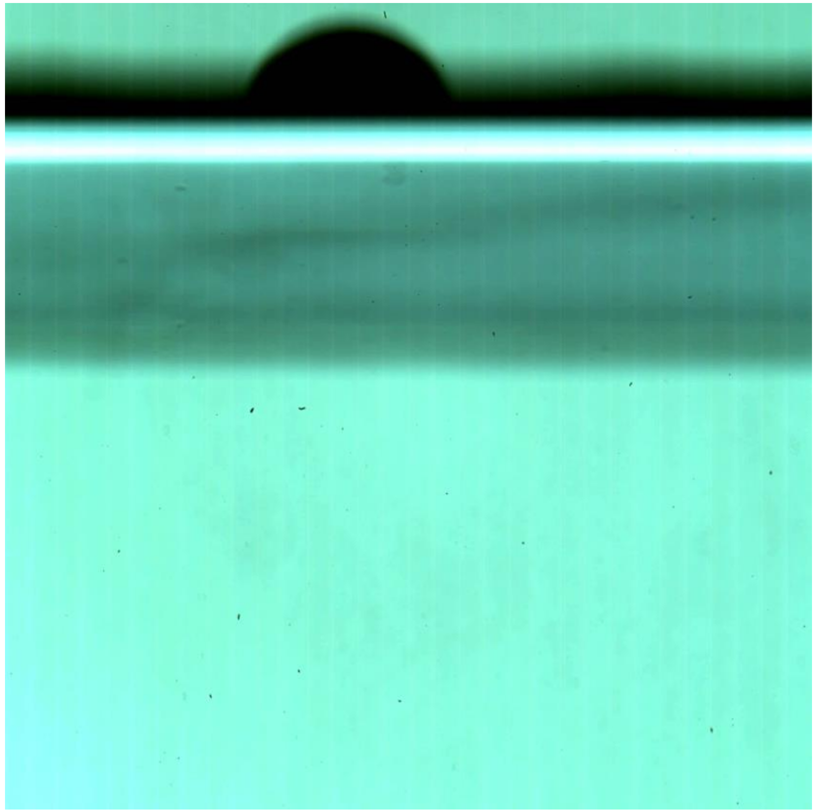

Vortex ring formation
- Velocity = 0.88 ms^{-1}

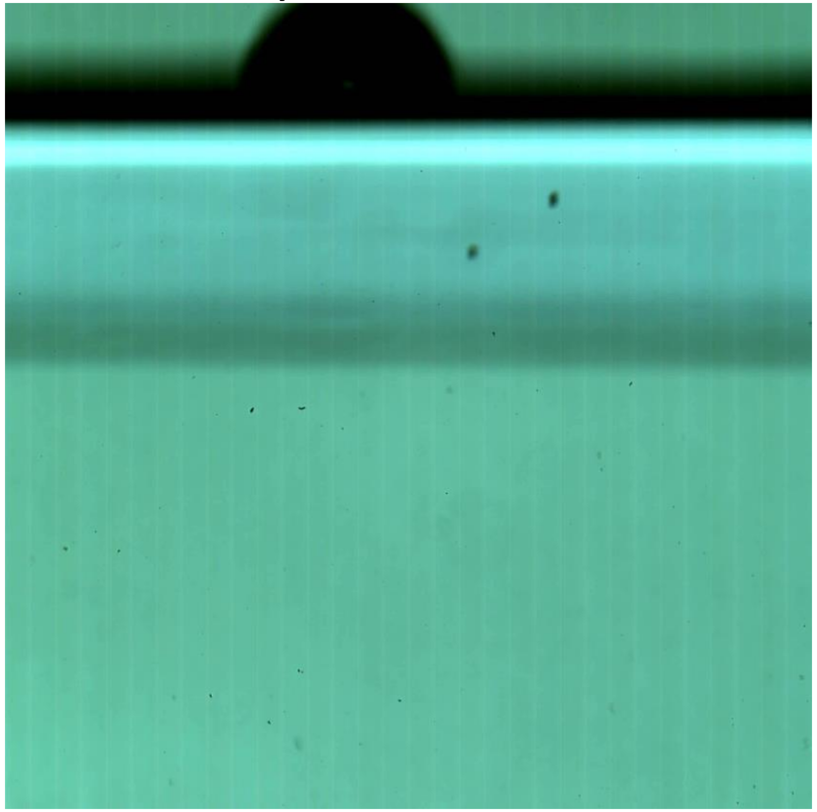

Central jet formation
- Velocity = 2.8 ms^{-1}

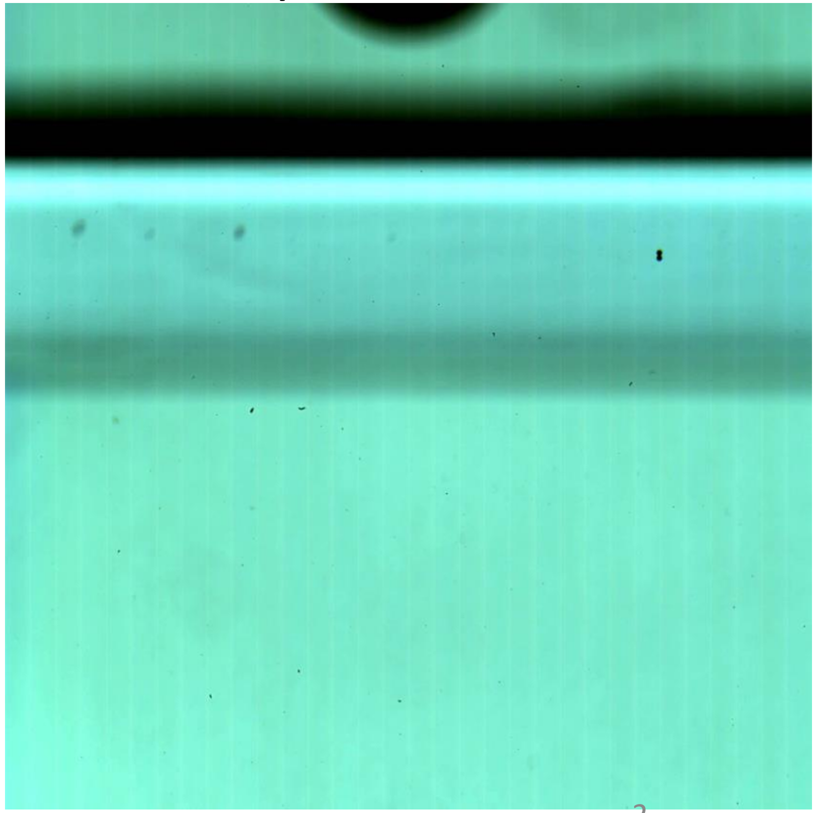

Background: Application of vortex rings

- During the formation of vortex ring it experience number of intermediate shapes from spherical to toroidal.
- These Intermediate can be frozen at controlled time point into particles by gelation or precipitation process.
- Electro spraying technique with their sizes well controlled from hundreds of microns to millimeters.
- Applicable to broad range of material.
- Bioencapsulation
- Catalytic reactions
- Structural materials construction

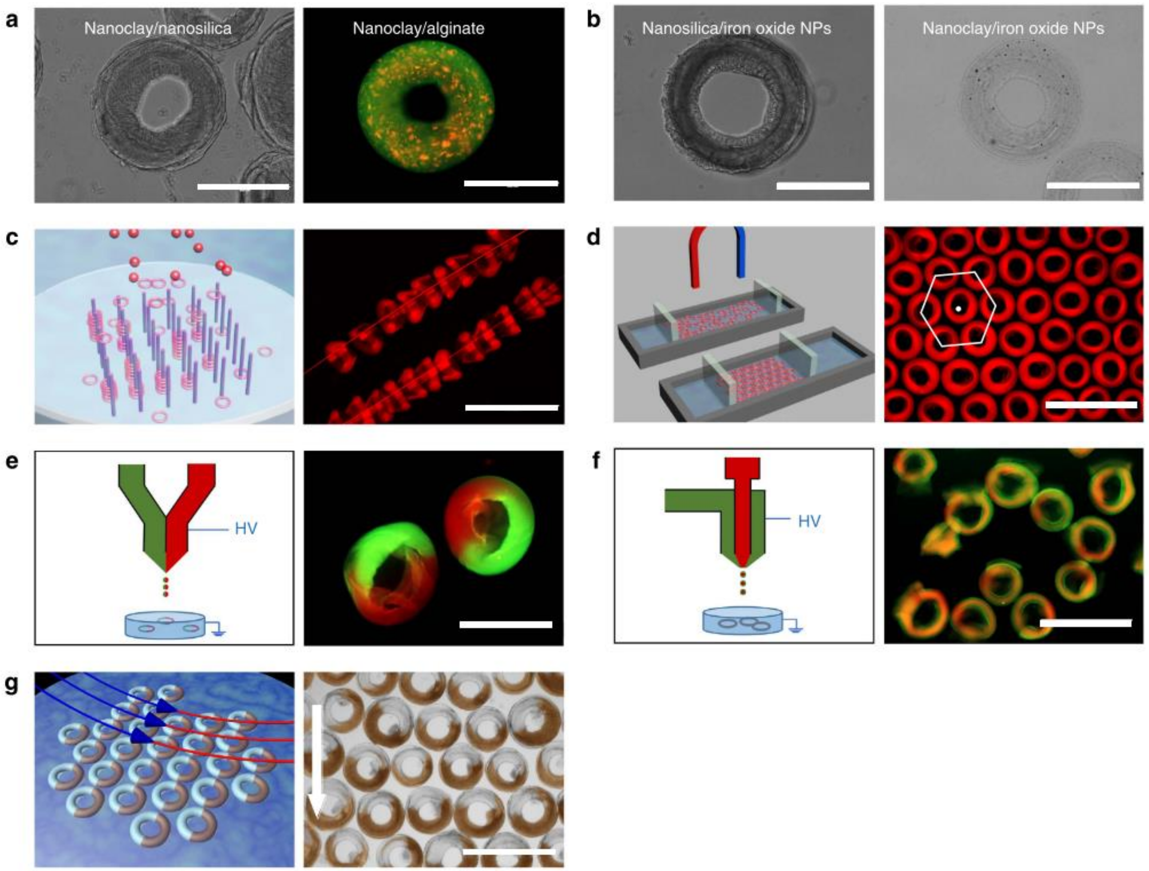

Figure 6 | Composite and assembly of donut-microVRP. (**a**) Donut-microVRP made from composite materials: nanoclay/nanosilica, nanoclay/alginate. (**b**) Magnetic donut-microVRP: nanosilica/Fe_3O_4 nanoparticles and nanoclay/Fe_3O_4 nanoparticles. (**c**) Schematic illustration of the assembly process and a microscopic image of the 1D structure made from nanoclay hydrogel donut-microVRP. (**d**) Schematic illustration of the assembly process and a microscopic image of the 2D structure made from magnetic nanoclay hydrogel donut-microVRP. (**e**) Schematic illustration of the nozzle design and a microscopic image of the Janus donut-microVRP. (red: alginate labelled with Alexa Fluor 594 dye; green: alginate labelled with Alexa Fluor 488 dye) (**f**) Schematic illustration of the nozzle design and a microscopic image of the core-shell donut-microVRP. (**g**) Directional assembly of the Janus magnetic nanosilica donut-microVRP; the arrow indicating the direction of the magnetic field. Scale bars, 400 μm (**a**,**b**); 2 mm (**c**,**d**,**f**); 1 mm (**e**,**g**).

An, D., Warning, A., Yancey, K. G., Chang, C.-T., Kern, V. R., Datta, A. K., … Ma, M. (2016). Mass production of shaped particles through vortex ring freezing. *Nature Communications*, *7*, 12401. https://doi.org/10.1038/ncomms12401

Background: Application of vortex rings

- During the formation of vortex ring it experience number of intermediate shapes from spherical to toroidal.
- These Intermediate can be frozen at controlled time point into particles by gelation or precipitation process.
- Electro spraying technique with their sizes well controlled from hundreds of microns to millimeters.
- Applicable to broad range of material.
- Bioencapsulation
- Catalytic reactions
- Structural materials construction

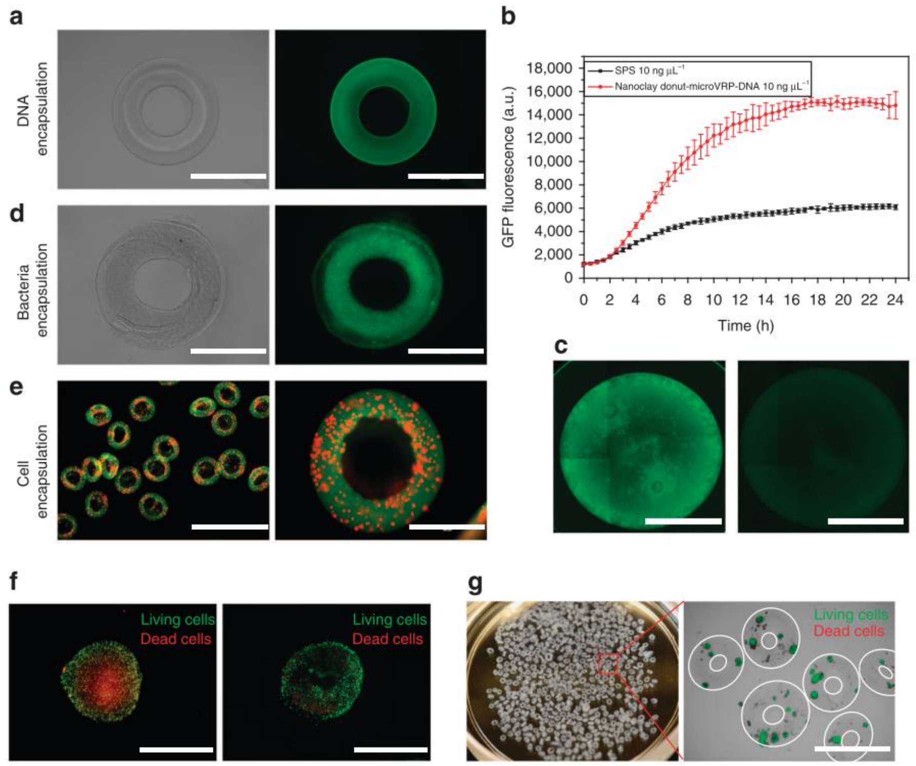

Figure 5 | Bioencapsulation applications using donut-microVRP. (**a**) A nanoclay hydrogel donut-microVRP encapsulating plasmid DNA: bright-field image and fluorescent image (stained with GelGreen). (**b**) Kinetic curve of the GFP fluorescence from cell-free protein production. Error bars in **b** represent one s.d. of the data away from the mean. (**c**) Fluorescent images of the reaction wells of cell-free protein production with (left) or without (right) nanoclay donut-microVRP. (**d**) A nanoclay hydrogel donut-microVRP encapsulating bacteria: bright-field image and fluorescent image (GFP-expressing *E. coli*). (**e**) Alginate hydrogel donut-microVRP encapsulating MDA-MB-231 cells that express Tomato red. (**f**) Cell viability test of the MDA-MB-231 cells encapsulated in an alginate spherical particle and an alginate donut-VRP, 4 days after encapsulation. The cells were stained with calcium-AM (green, live) and ethidium homodimer (red, dead). (**g**) Rat pancreatic islets encapsulated in the alginate donut-VRP. Scale bars, 400 μm (**a**, **d**, **e** right panel); 3 mm (**c**); 2 mm (**e** left panel, **f**, **g**).

An, D., Warning, A., Yancey, K. G., Chang, C.-T., Kern, V. R., Datta, A. K., … Ma, M. (2016). Mass production of shaped particles through vortex ring freezing. *Nature Communications*, *7*, 12401. https://doi.org/10.1038/ncomms12401

Problem Statement

- Effect of pool depth?
- Vortex ring formation
  - In pool of different depths?

- How will pool depths effect the dynamics of vortex ring?

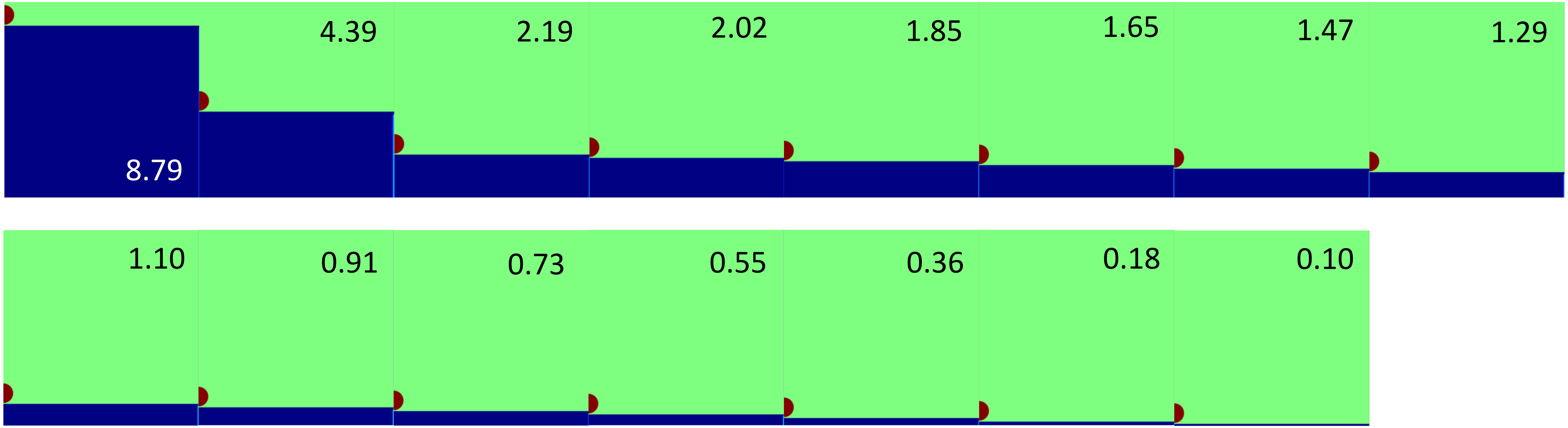

Problem Statement

- High-speed imaging & numerical simulation to characterize the dynamics in different pool depths.
- This will allow us to better control the shape of the particles and eventually produce sophisticated hierarchical materials.

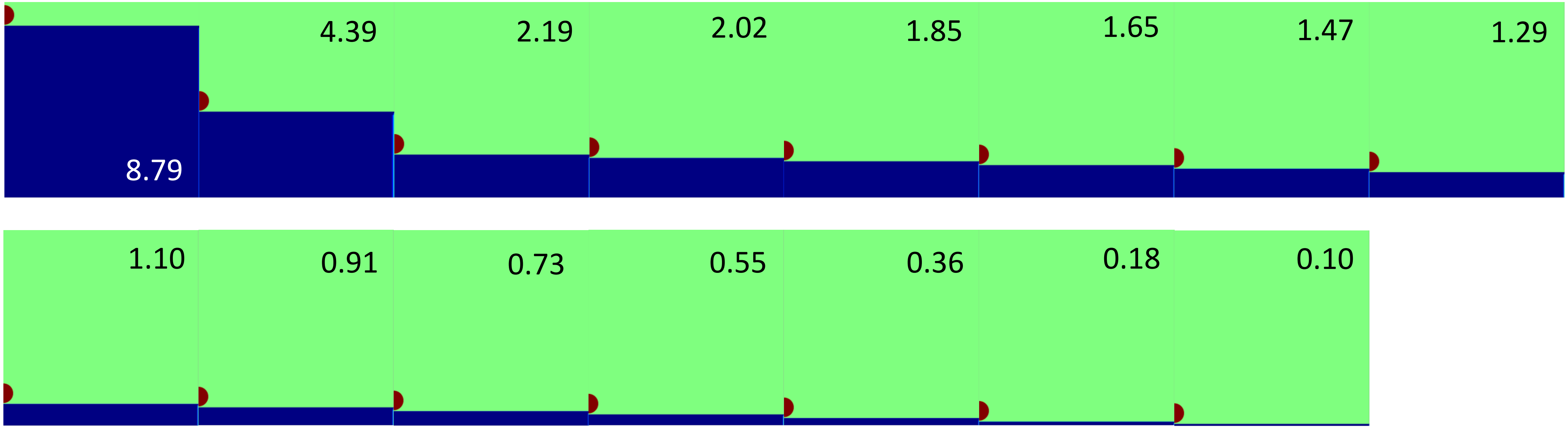

Non-dimensional parameters: Drop impact on a pool of same liquid

- **Reynold number:**

  Relates inertial forces to viscous forces

$$\mathrm{Re} = \frac{\rho_l \times V \times D}{\mu_l}$$

- **Weber number:**

  Relates inertial forces to surface tension force

$$We = \frac{\rho_l \times V^2 \times D}{\sigma}$$

- **Froude number:**

  Relates inertial forces to gravitational forces

$$Fr^2 = \frac{V^2}{g \times D}$$

- **Geometrical aspect ratio:**

  Ratio of pool depth to drop diameter

$$h^* = h / D$$

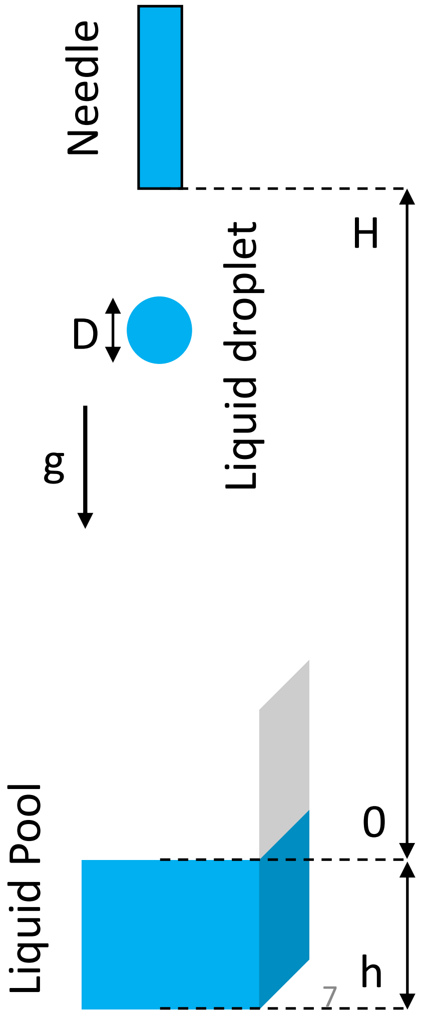

Non-dimensional parameters: Drop impact on a pool of same liquid

- **Time scale:**

  The time vortex ring take to move one drop diameter defined as:

$$t^* = t/(D/V)$$

- **Length Scale:**

  The radial coordinate and axial coordinates are nondimensionalized by drop diameter

$$r^* = r(t)/D$$
$$z^* = z(t)/D$$

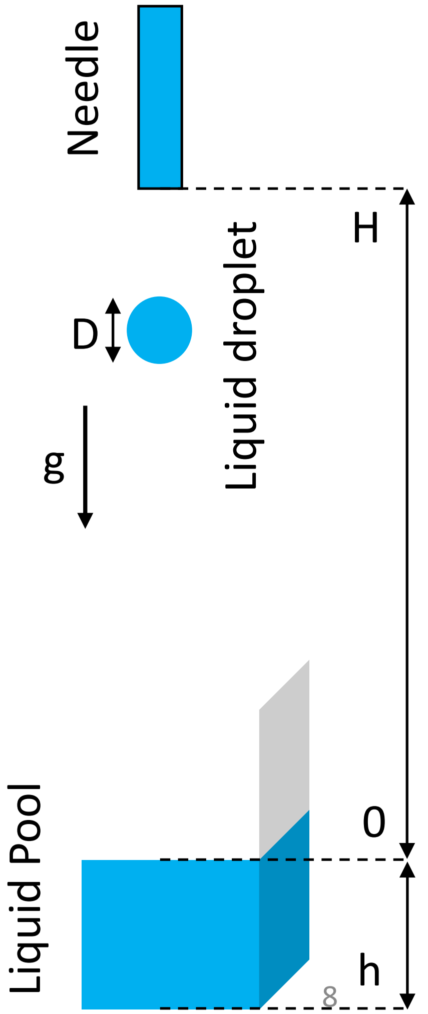

Symbolic representations

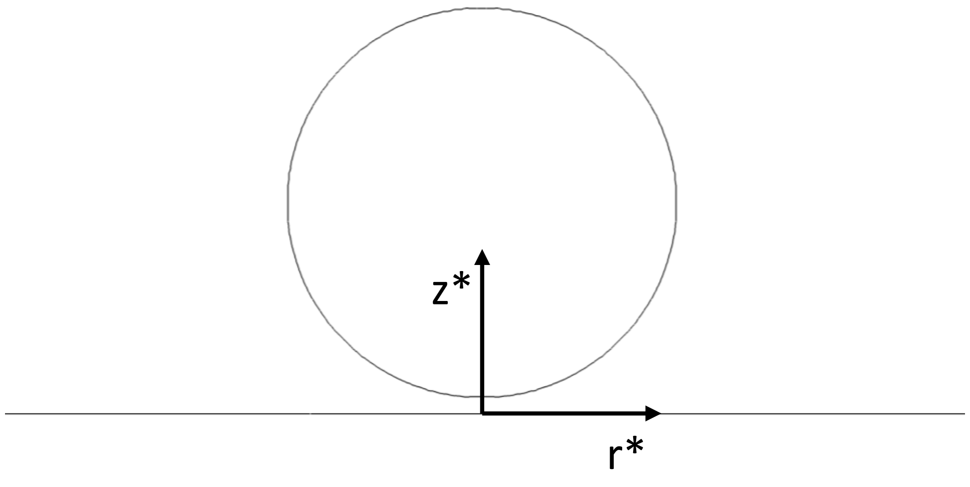

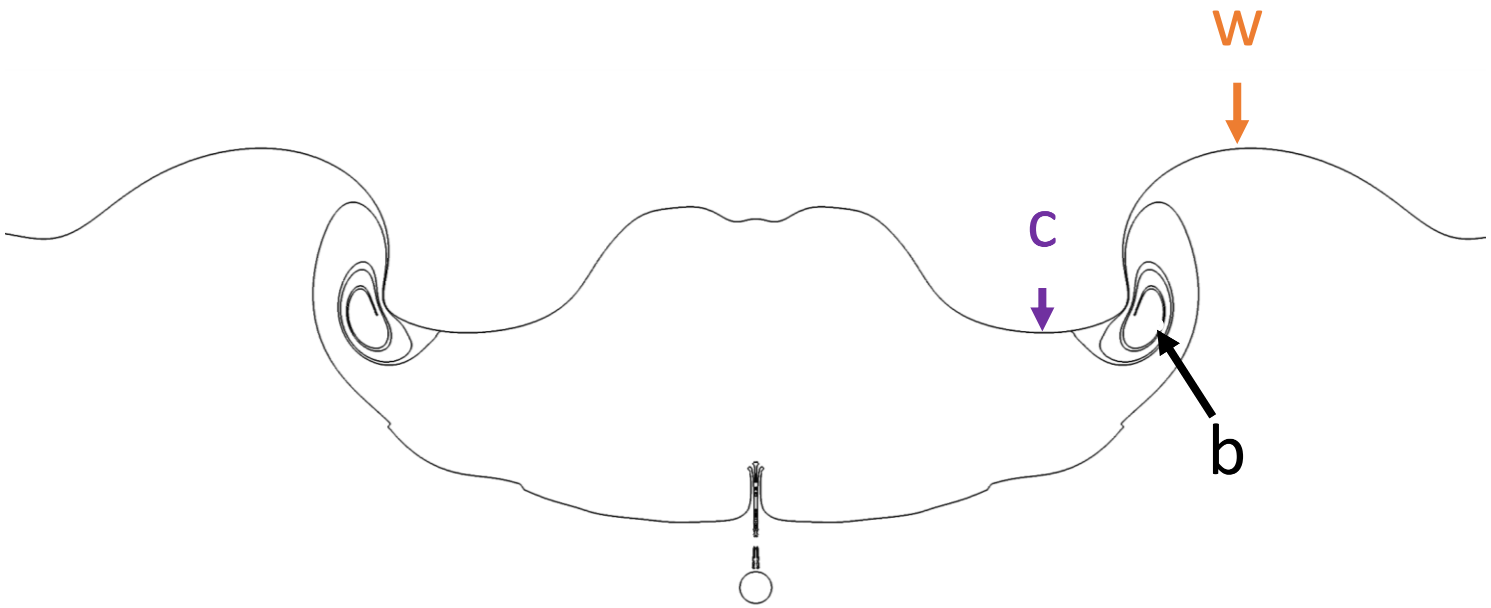

Vortex ring (b); Crater depth (c); Wave swell (w);

Vortex ring formation

- Drop & Pool liquid: 30% glycerin solution
- Velocity = 0.99 ms^{-1}
- Drop Diameter = 2.73 mm
- Reynolds = 1300
- Weber = 41
- Froude = 6
- Pool depth: h* = 4.39, 2.19, $\boxed{1.01}$, 0.91, 0.73, 0.55, 0.36, 0.18, 0.1

Vortex ring formation: Two views experiments

Positive View

Camera angle is ≈+1º to 2º degree from the horizontal plane

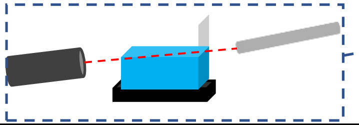

Negative View

Camera angle is ≈-1º to 2º degree from the horizontal plane

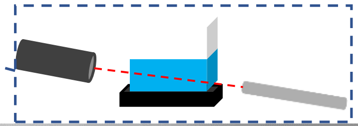

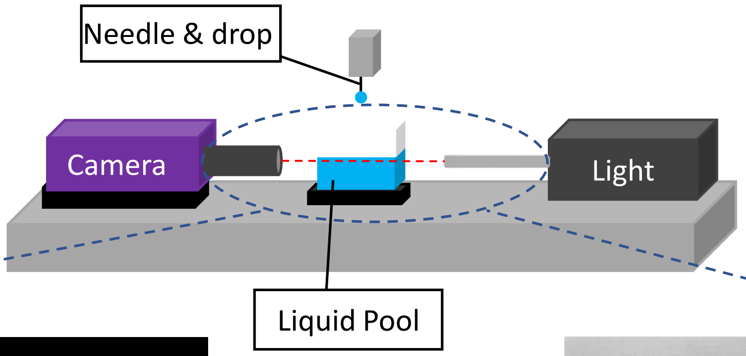

$V = 0.99\ ms^{-1}$

$h^{*} = 1.01$

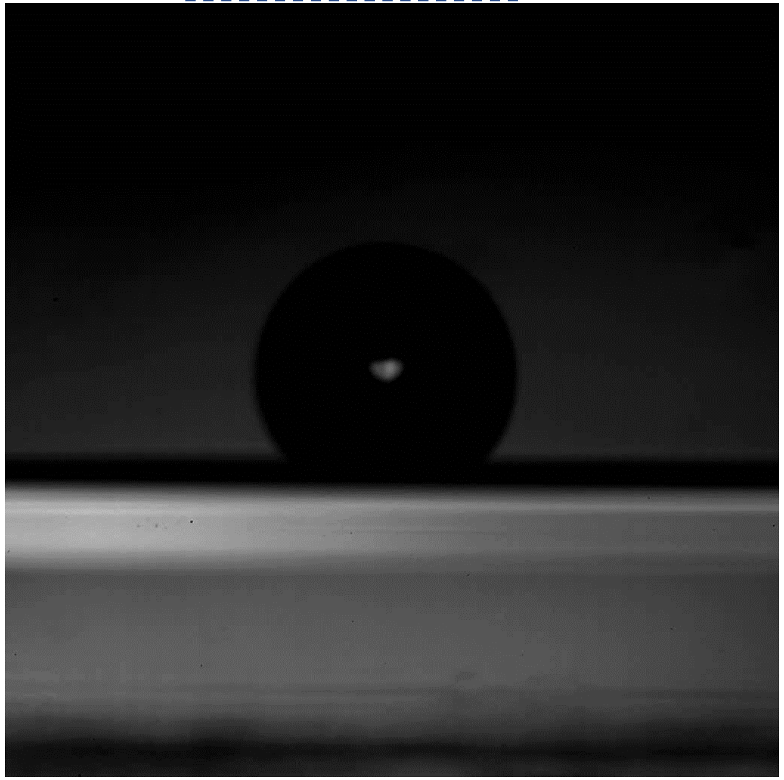

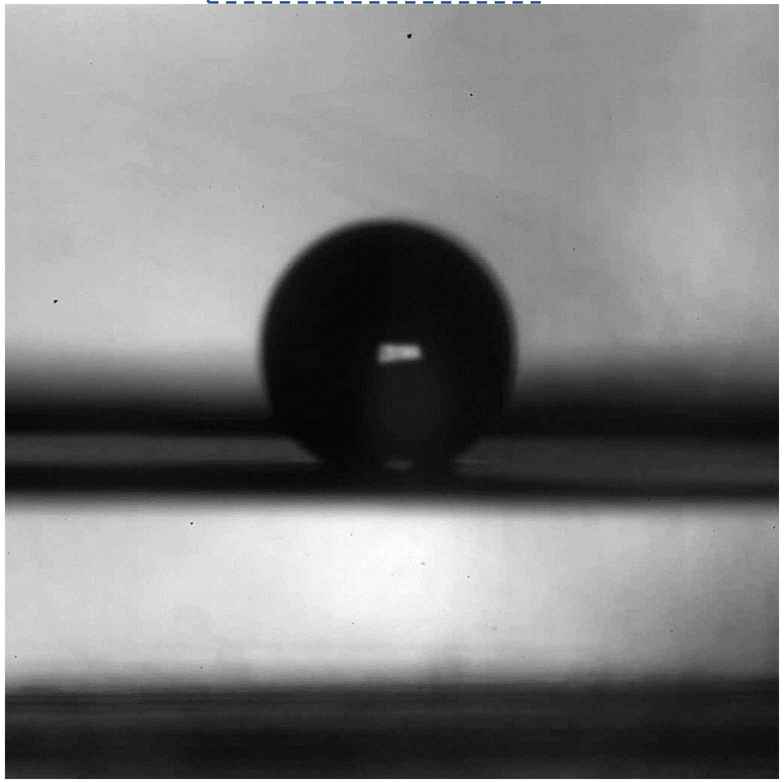

Vortex ring formation: Trajectory merging of two views

Positive View

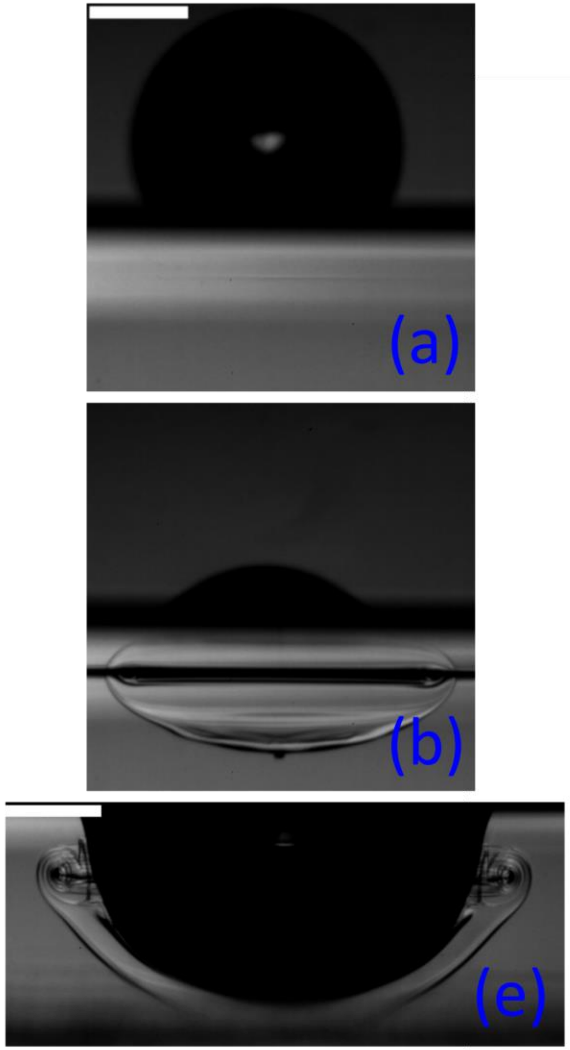

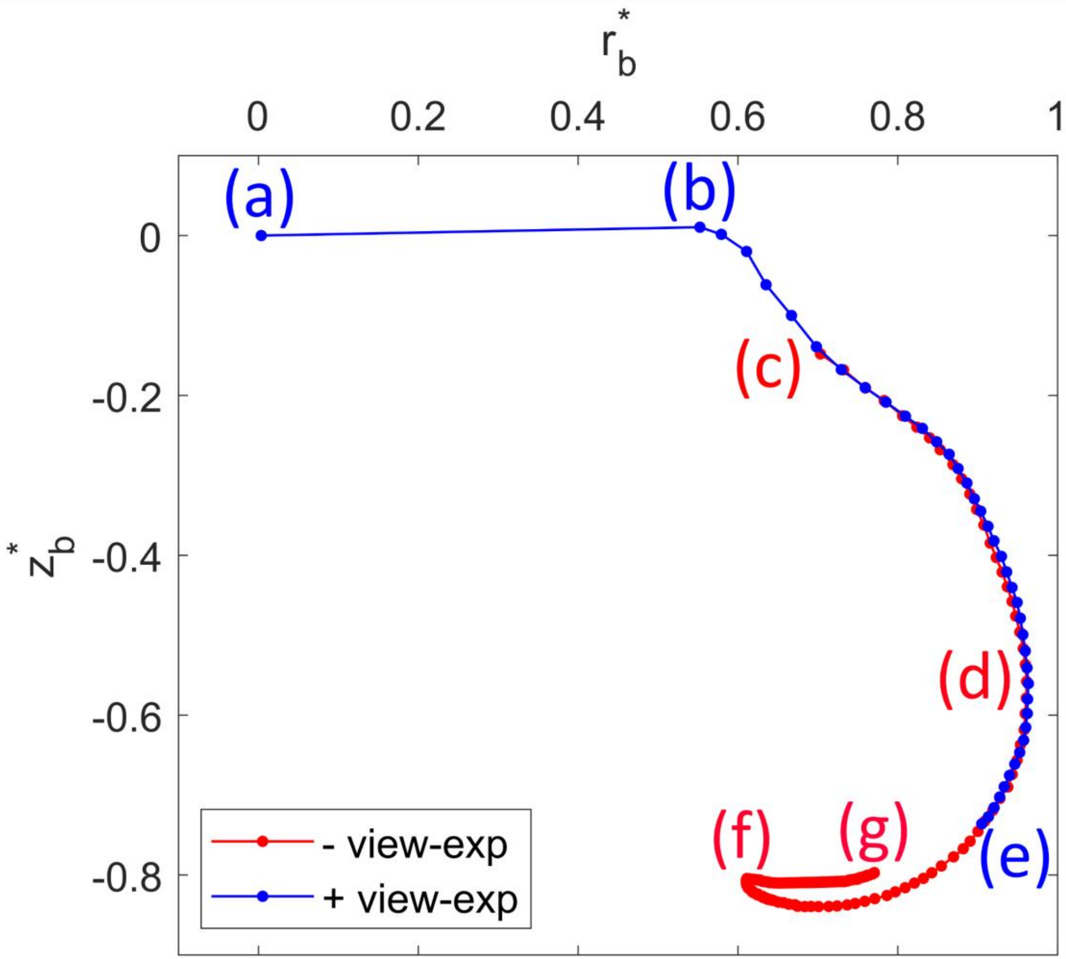

Negative View

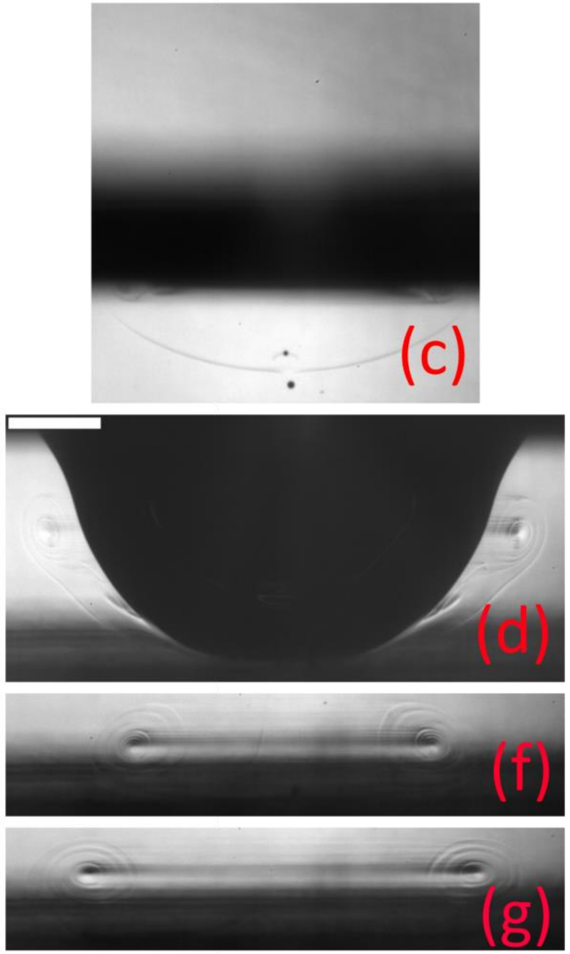

Vortex ring formation: Trajectory deep & shallow pools

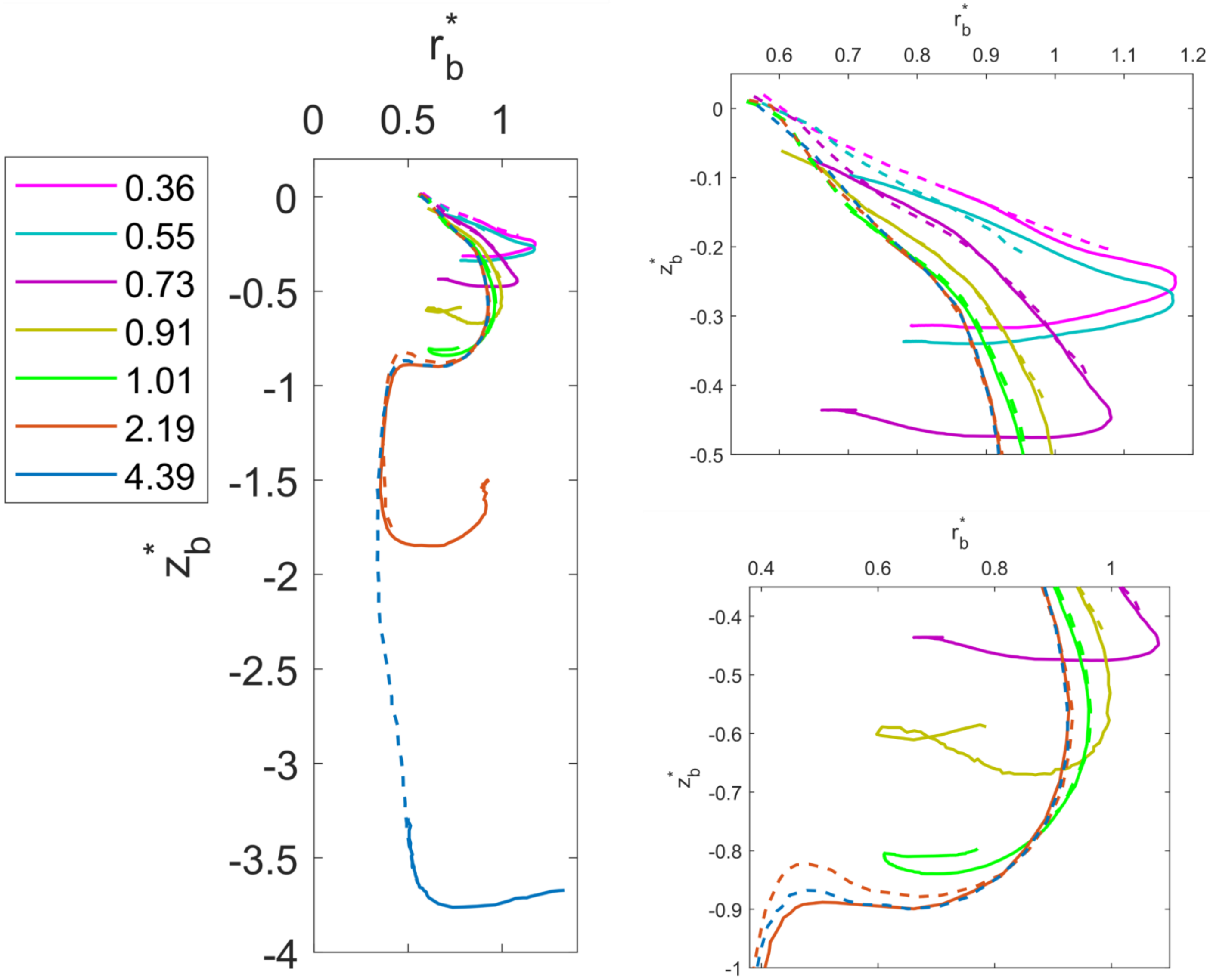

Numerical Simulation: Numerical setup

- Drop & Pool liquid: 30% glycerin solution
- Velocity = 0.99 ms^{-1}
- Drop Diameter = 2.73 mm
- Reynolds = 1300
- Weber = 41
- Froude = 6
- Pool depth: h* = $\boxed{1.01}$
- Systematic decrease of h* = 8.79, 4.39, 2.19, 2.02, 1.85, 1.65, 1.47, 1.29, 1.10, 0.91, 0.73, 0.55, 0.36, 0.18, 0.10

Numerical setup: Simulation domain

- Minimum level of refinement = 7
- Maximum level of refinement = 12
- No of cells per drop diameter = 409

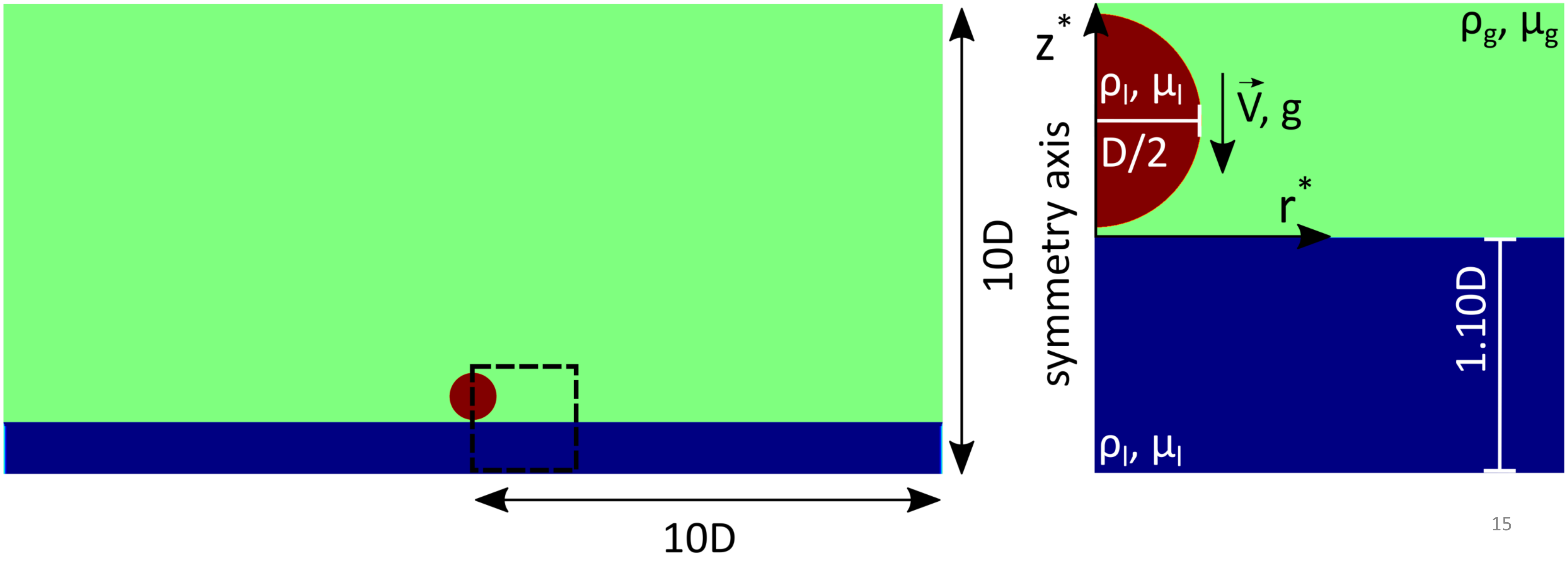

Tracking of vortex ring trajectory: Validation

Tracking: vortex ring

- Pool depth: h* = 1.01

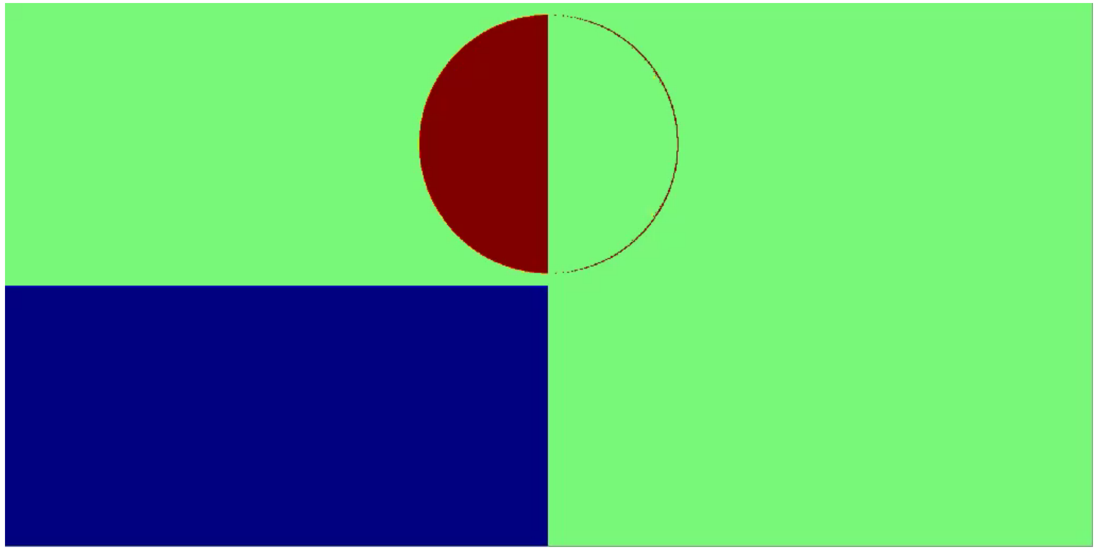

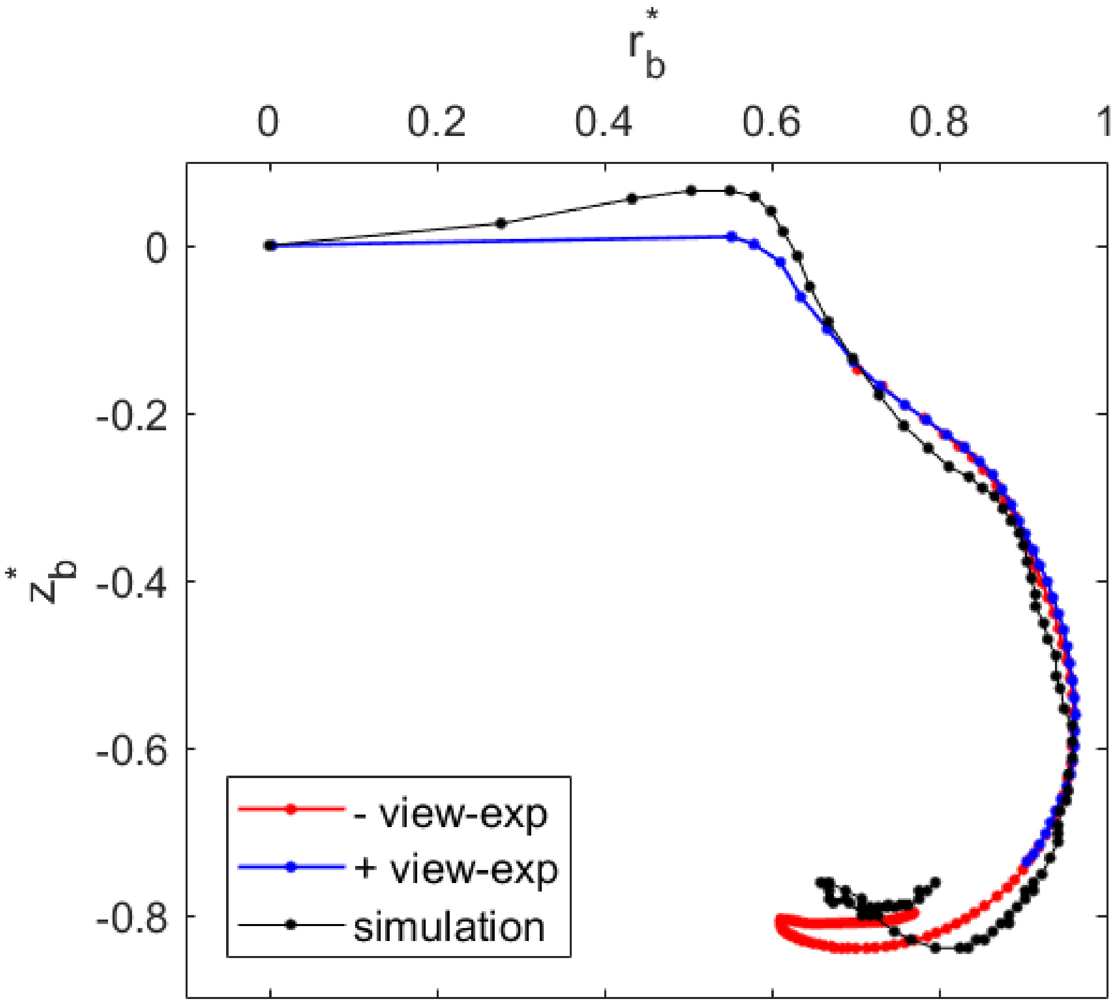

Three regimes: Two transitions in vortex ring dynamics

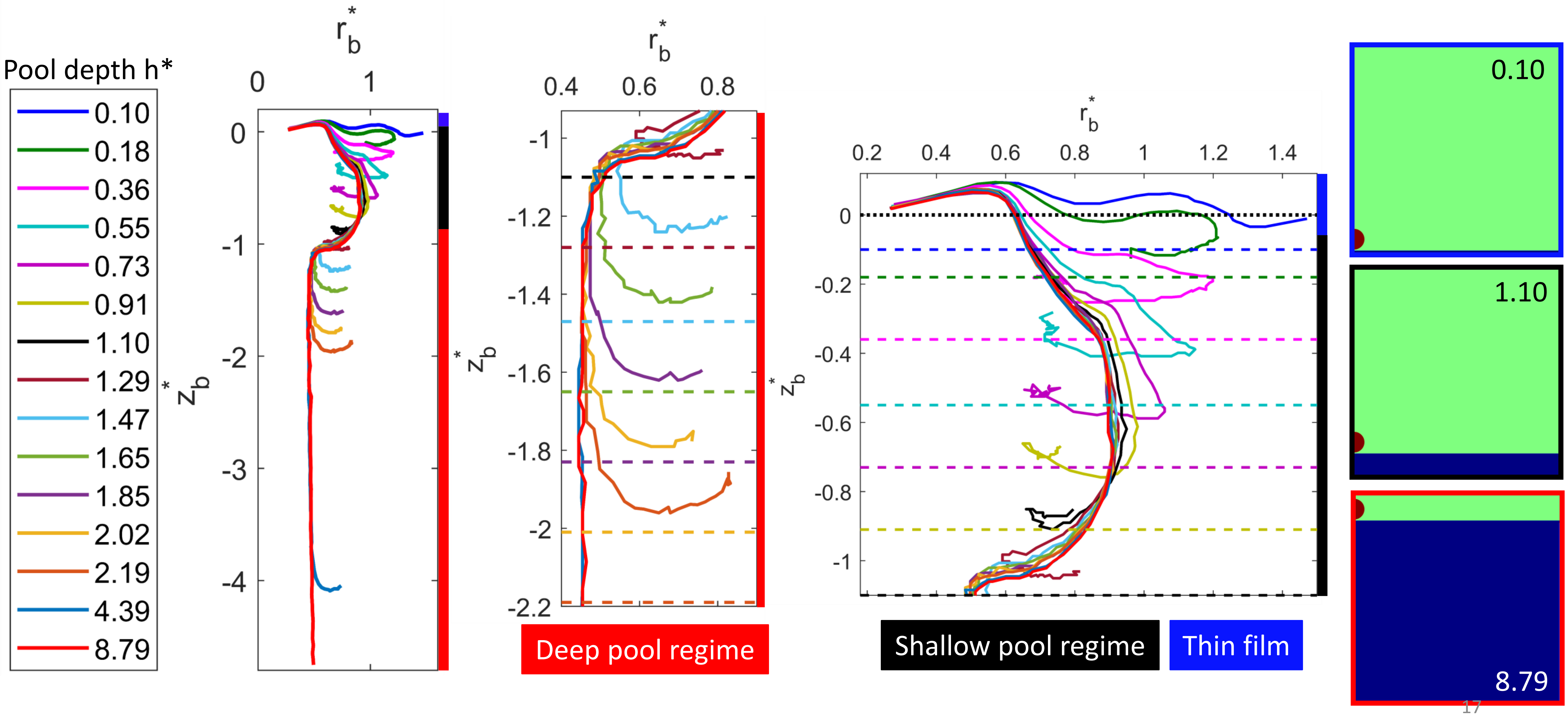

Evolution of crater depth and vortex ring diameter

Pool depth: h* = 1.01

Different pool depth

Vortex ring diameter

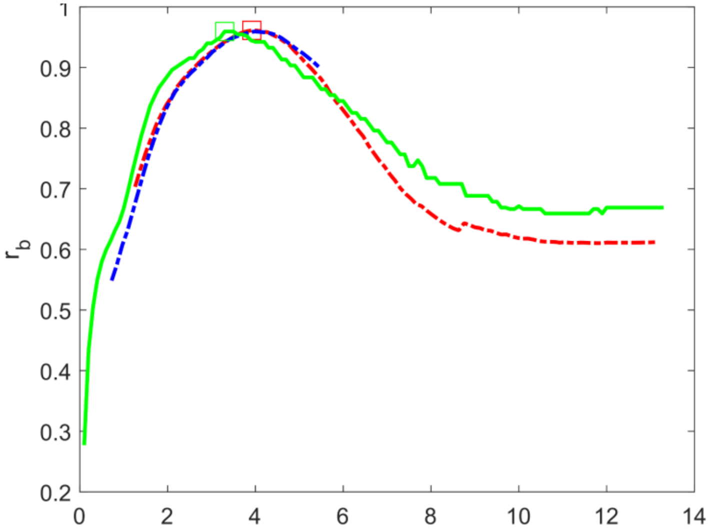

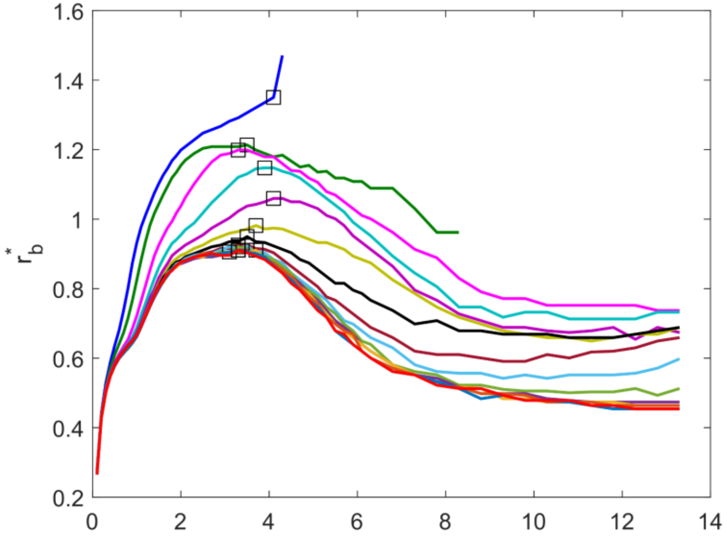

Crater depth

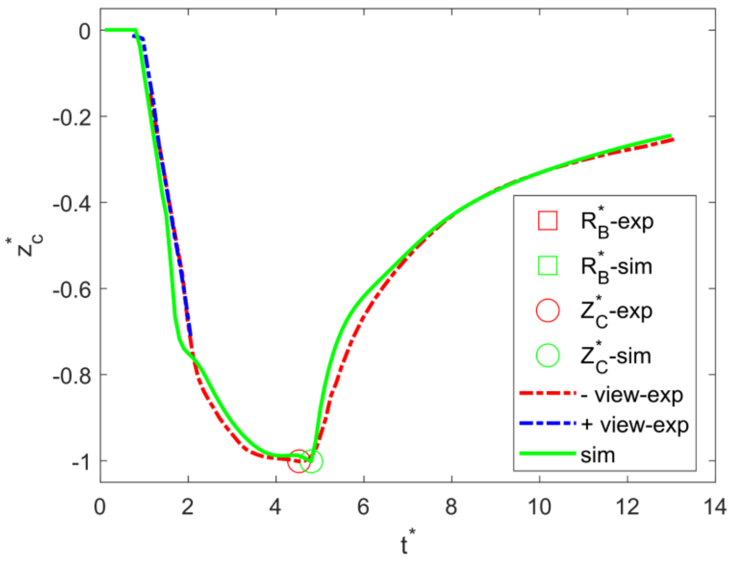

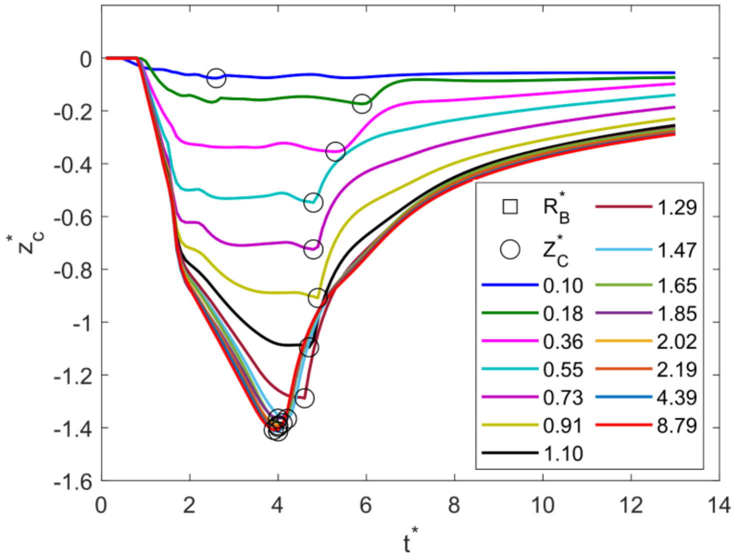

Maximum Vortex ring diameter and crater depth

Maximum vortex ring diameter

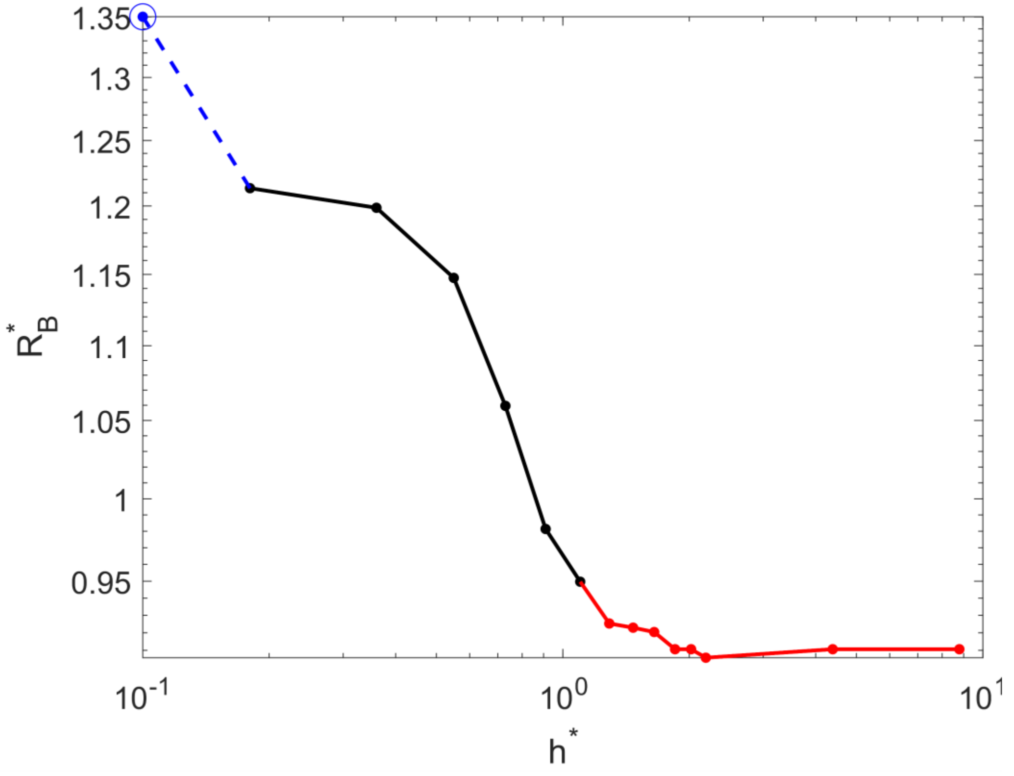

Maximum crater depth

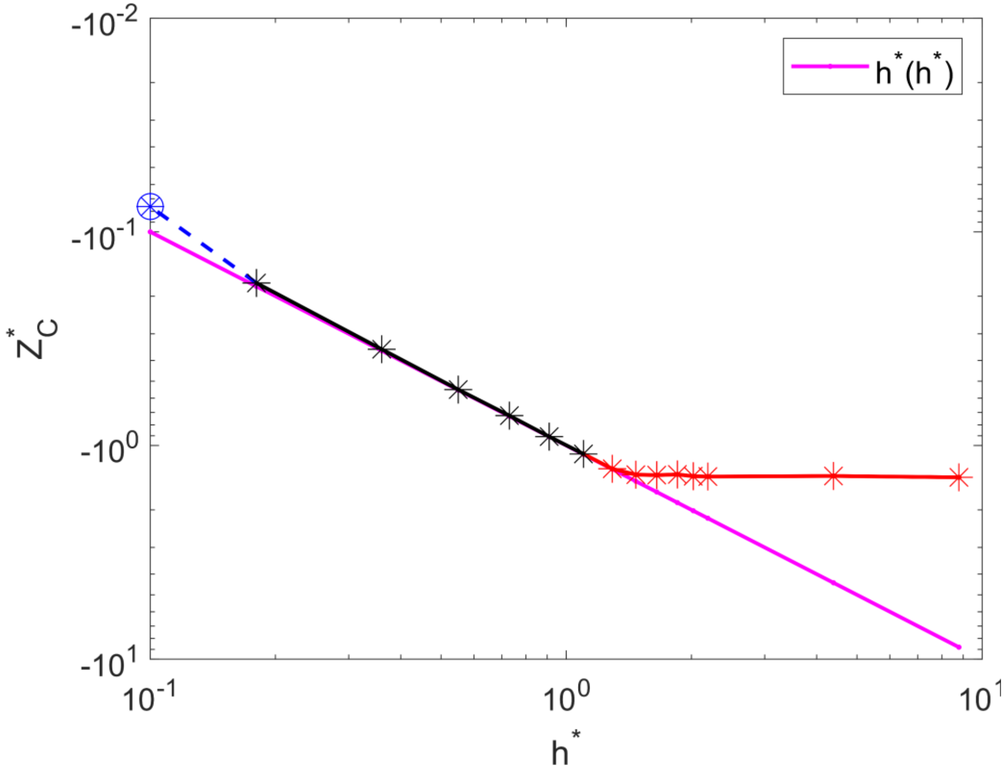

Deep pool regime

Shallow pool regime

Thin film

Maximum Vortex ring diameter and crater depth

Time of maximum vortex ring diameter

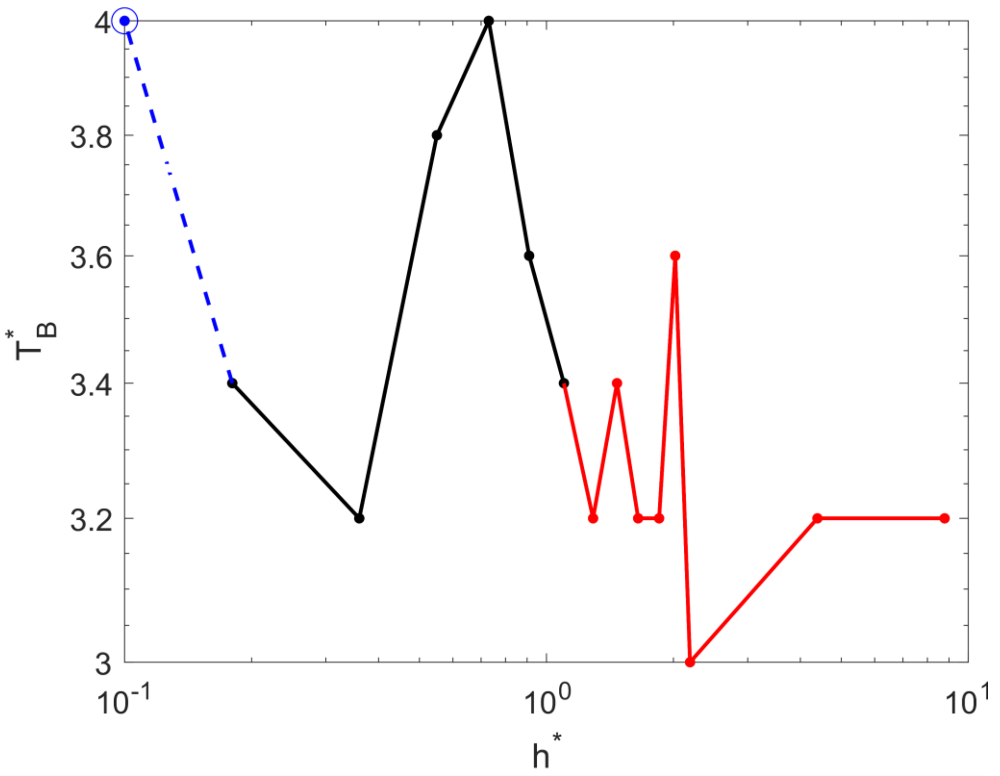

Time of maximum crater depth

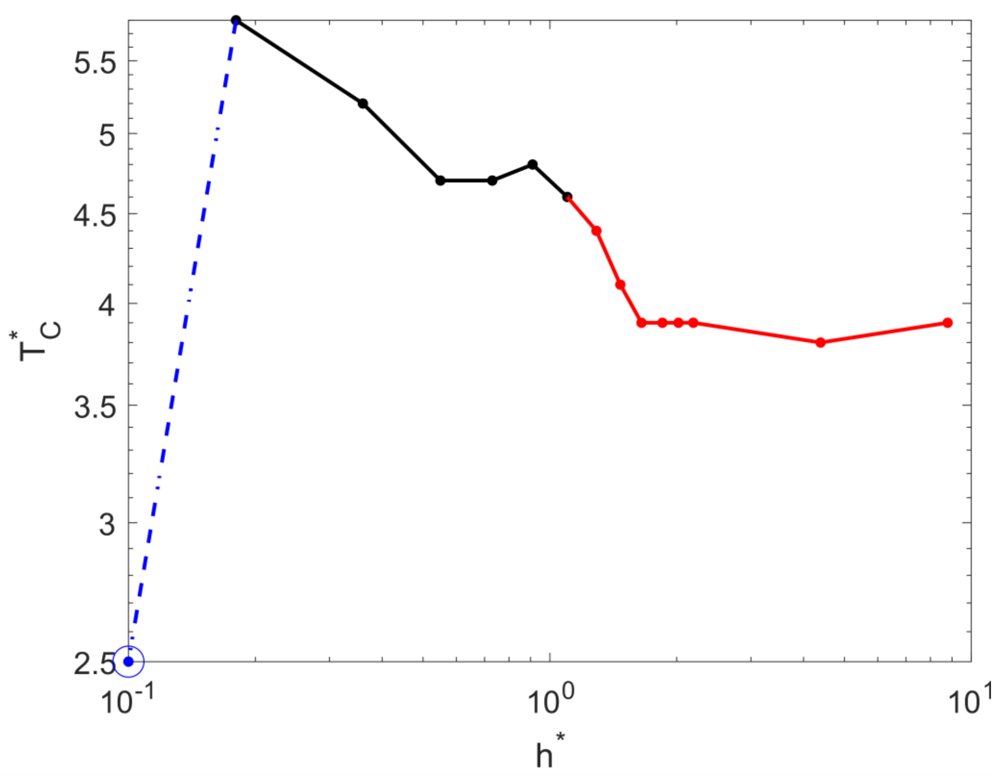

Deep pool regime

Shallow pool regime

Thin film

Correlation between crater depth and vortex ring

Interface profiles for h*: 8.79

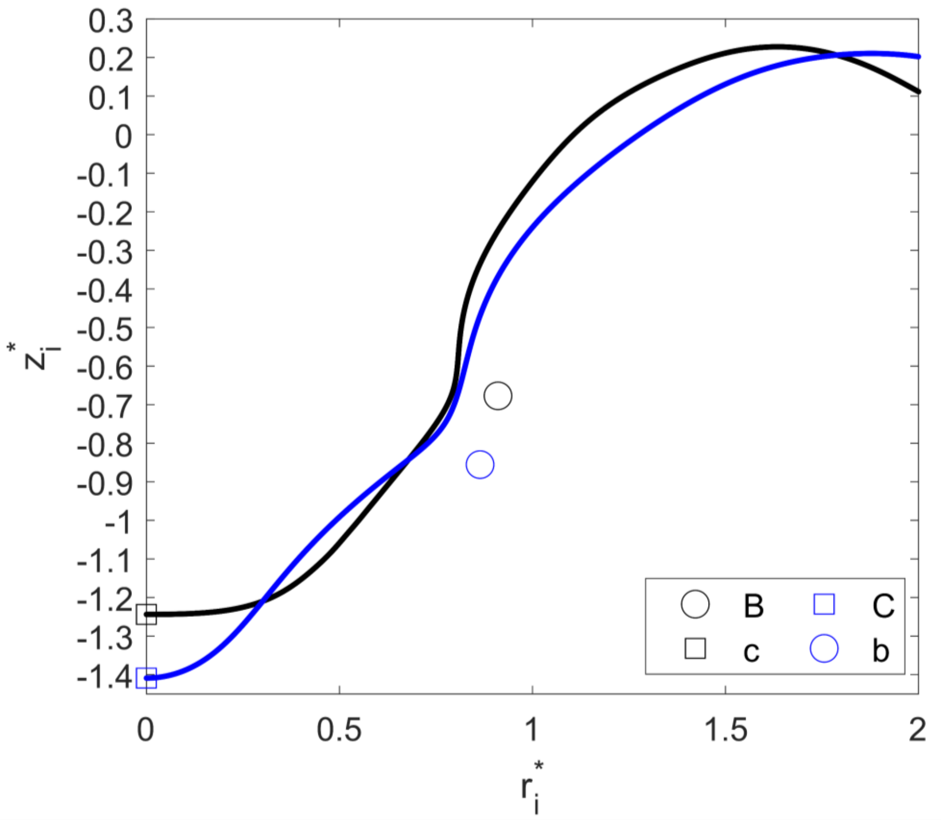

T^*_B: 3.2 & T^*_C: 3.9

Interface profiles for h*: 1.10

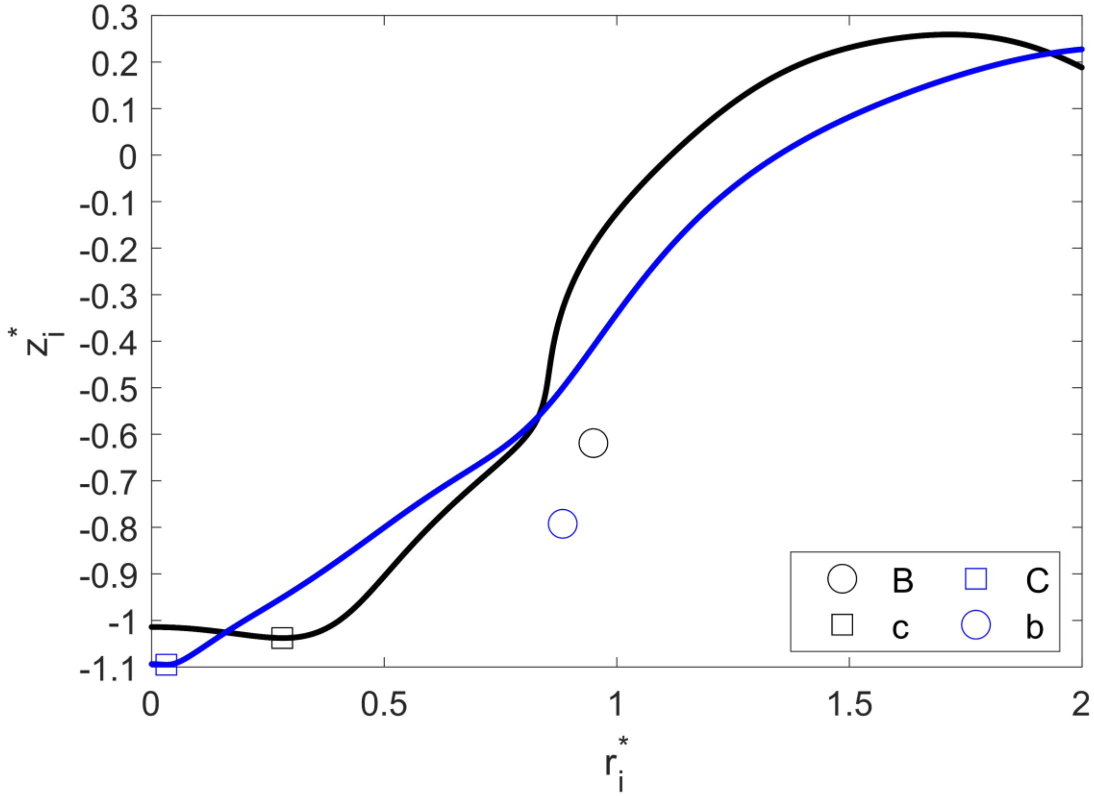

T^*_B: 3.4 & T^*_C: 4.6

Black: Maximum vortex ring diameter (R^*_B); Blue: Maximum Crater depth (Z^*_C);

Correlation between crater depth and vortex ring

Evolution of wave swell height and vortex ring diameter

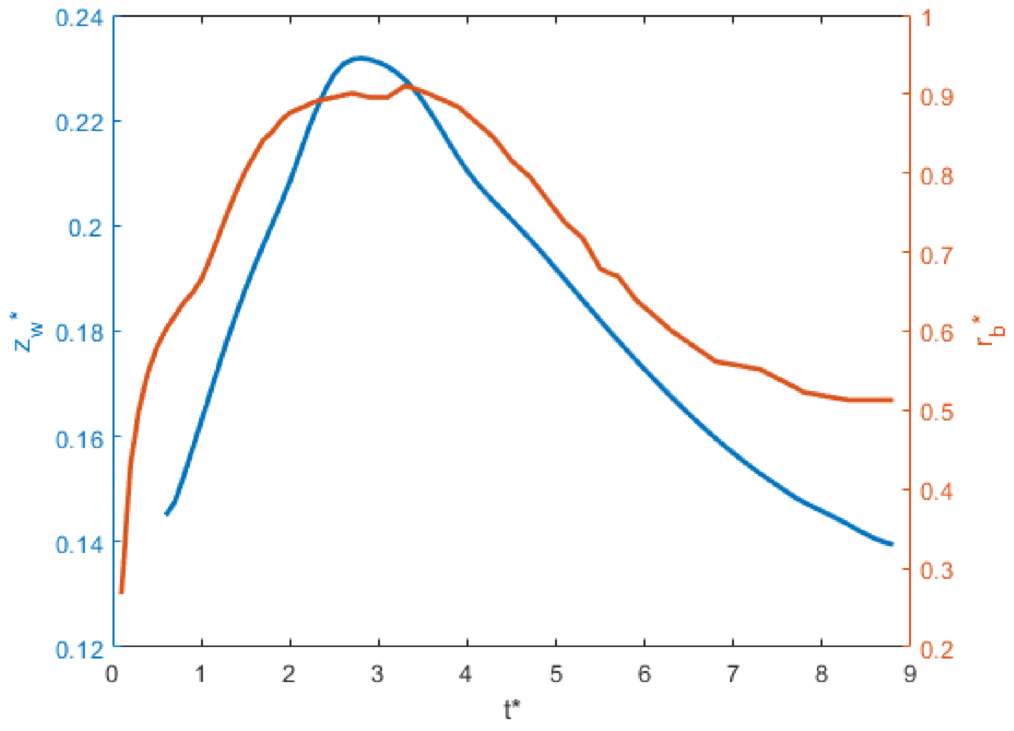

h*: 8.79

Maximum wave swell height and vortex ring diameter as a function of pool depth

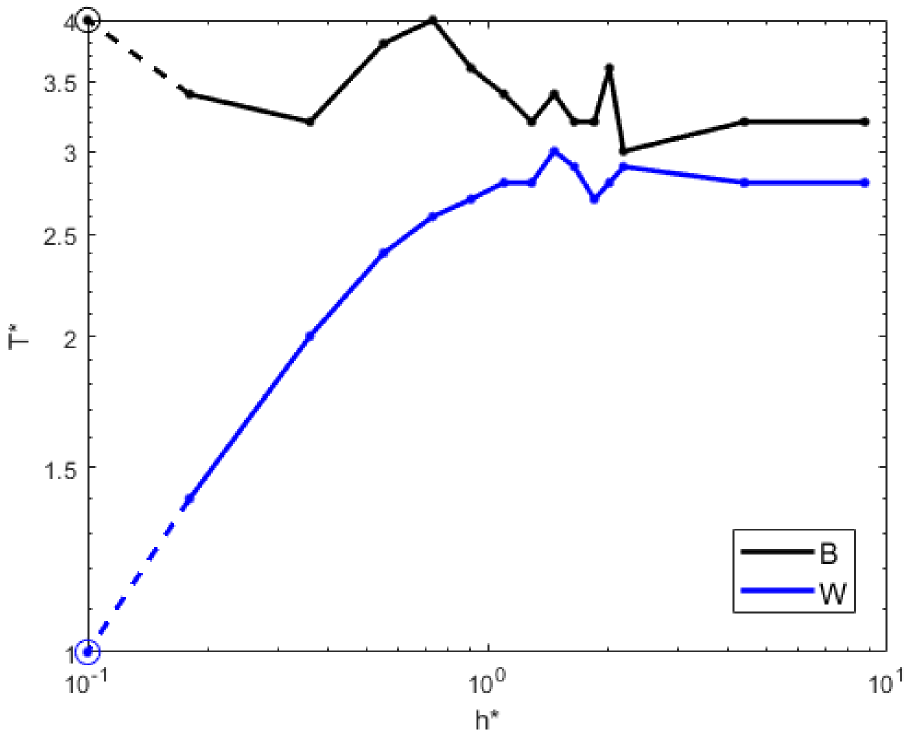

Kinetic Energy

We = 41

Pool depth h*

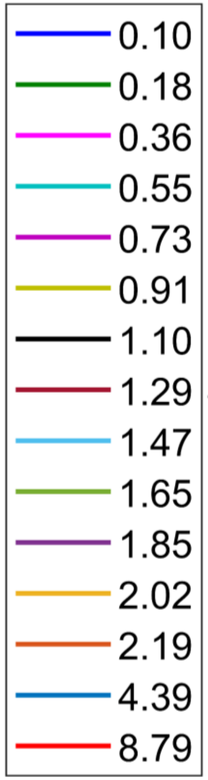

Vertical direction

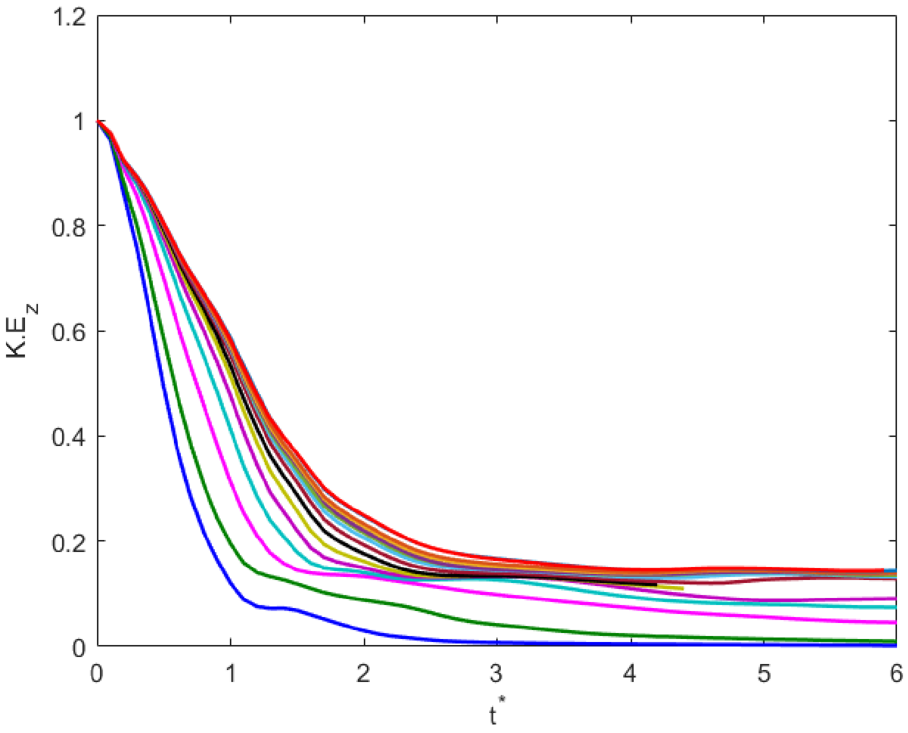

Radial direction

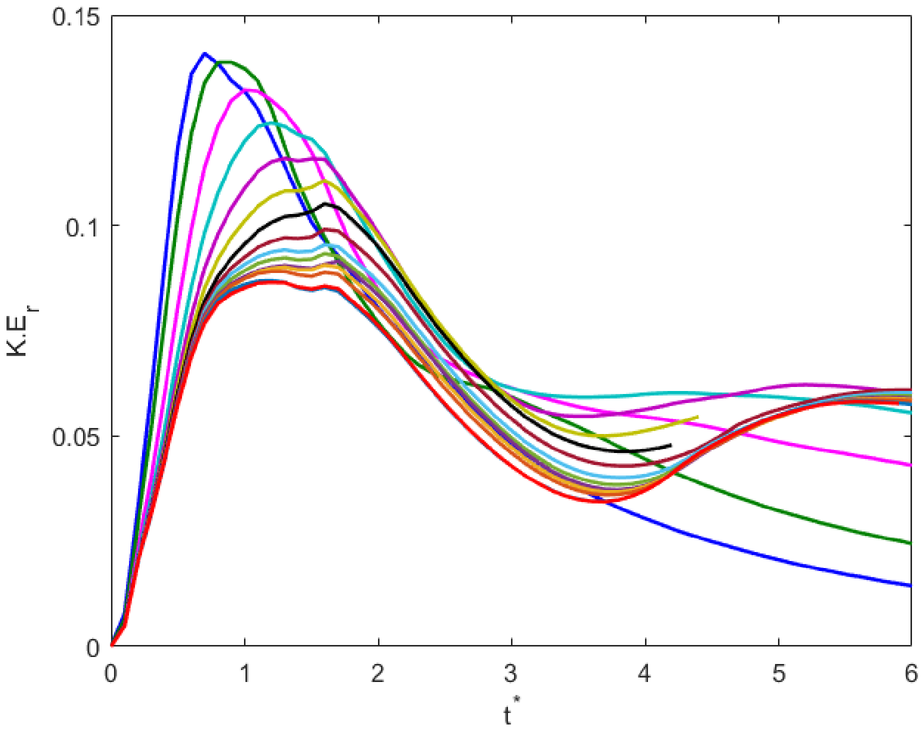

Scaling

Time of maximum crater depth

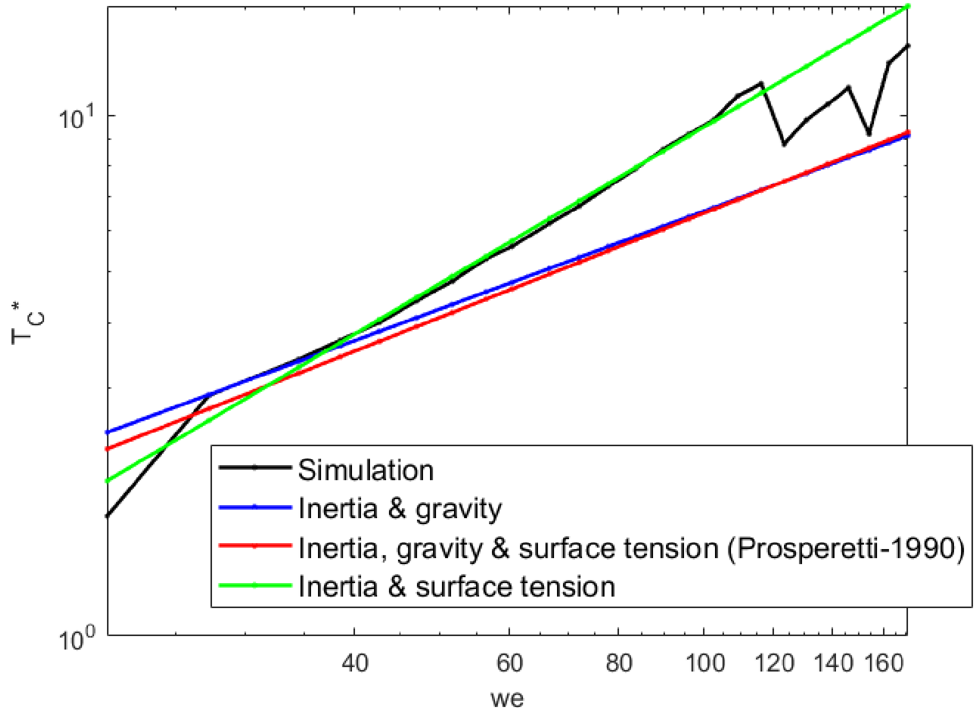

h*: 8.79

Maximum crater depth

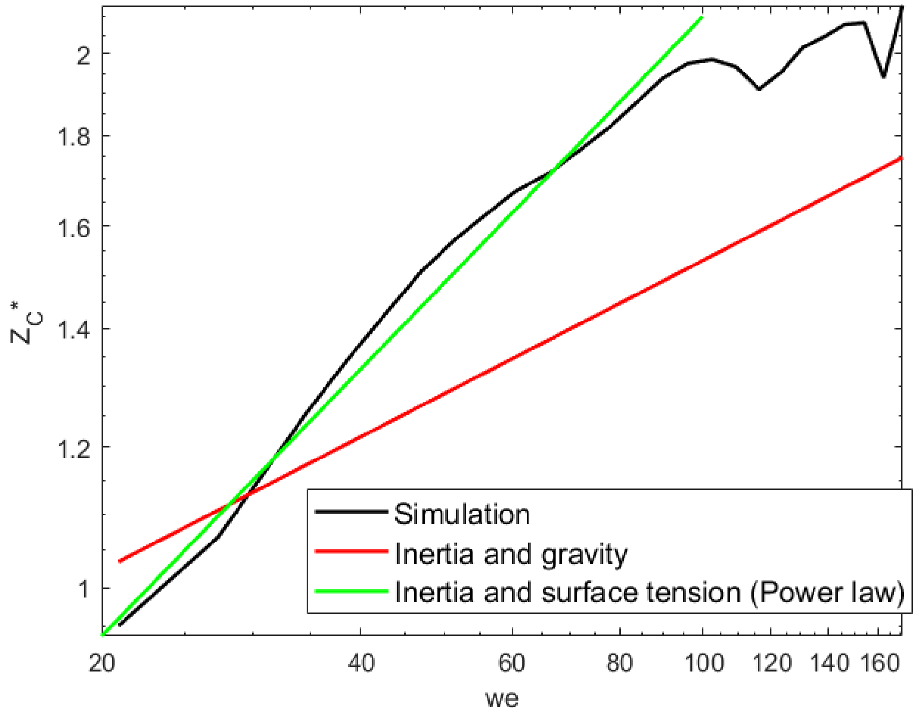

Outlook

- Calculation of surface energy and viscous dissipation to further validate our arguments
- Scaling laws for different weber number developed on the basis of inertia, capillarity and gravity.
- The effect of pool depth than can further be studied for full parameter space of velocity.

Acknowledgments

I would like to acknowledge Basilisk Scholarship and funding from Xi'an Jiaotong University to cover expenses of my Paris trip to attend the Basilisk/Gerris Users' Meeting 2019.

Thank you for your attention!

Any questions, comments, or suggestions are welcome.